Gas Turbine Dynamic Dynamometry: A New Energy Engineering Laboratory Module

Zhiyuan Yang[1] (yangz@msoe.edu),
Hope L. Weiss[2] (weiss@msoe.edu),
Matthew J. Traum[3] (traum@msoe.edu)

Mechanical Engineering Department
Milwaukee School of Engineering

Abstract

To integrate energy topics into STEM curricula, an archive of "Energy Engineering Laboratory Modules" (EELMs) is being developed by collaborating faculty and students at the Milwaukee School of Engineering (MSOE). EELMs facilitate spiral insertion of energy engineering experiments into college and high school STEM courses. By making innovative use of inexpensive equipment, EELMs facilitate near-ubiquitous accessibility to energy curricula, even for instructors with limited resources.

Gas turbines are paramount to modern energy production and transportation, and this critical technology will continue its prominence as we pursue a renewable energy future. Exposure to gas turbines through hands-on experiments could provide meaningful content for a range of STEM courses. However, prohibitively expensive commercially available educational test stands preclude gas turbine experiments from all but specialized engineering programs. Moreover, even if gas turbine hardware is available, specialized dynamometer and data acquisition equipment are needed to evaluate performance. Alternatively, virtual laboratories can offer rich simulated experiences to promote learning, but they lack the stimulating tactile and tangible learning experiences applied experiments provide.

We describe a method to accurately measure and predict the mechanical power output of a gas turbine using the rational inertia of the turbine's spinning components and friction in its bearings as the load. The turbine's time response to Dirac load inputs and its no-load responses to compressed air input over a range of pressures are measured. This technique, called dynamic dynamometry, requires only an inexpensive optical tachometer, a digital video recorder, and free image capture software for data acquisition. Turbine power-versus-angular-velocity curves are produced, which can be used for design, additional analysis, and teaching. An additional benefit of this technique is that turbine rotational inertia is determined independently of knowing the rotor's geometry. So, the experiment can be completed without dismantling the turbine; or, if desired, the measured rotational inertia can be independently verified by disassembling the turbine to measure internal component geometry and mass.

In addition to obvious applications for anchoring classroom discussions in physics, mechanical dynamics, fluid mechanics, and thermodynamics; this exercise offers unexpected teaching

[1] Undergraduate Research Assistant
[2] Assistant Professor
[3] Assistant Professor, Corresponding Author

opportunities for courses including Numerical Methods, Experimental Methods, and Statistics. Coarse data acquisition frequency necessitates conditioning the raw power-versus-angular-velocity data to distinguish meaningful, accurate performance curves. Moreover, outliers can be identified and eliminated via statistical techniques.

Introduction

Increasing energy-focused education is important to meet the growing demand for sustainability-conscious technical professionals. Gas turbines are paramount to modern energy production and transportation, and this critical technology will continue its prominence as we pursue a renewable energy future.[1] Thus, within STEM curricula, a need exists to provide practical, hands-on training in gas turbine systems. In parallel, however, a pragmatic need remains to balance energy-focused training with classical engineering and science fundamentals while keeping institutional costs manageable. New energy course content and the laboratory apparatuses used to deliver it must be carefully evaluated and integrated so as not to overburden STEM programs or curricula.

Three approaches predominate the instruction of gas turbine systems in current engineering curricula. First, gas turbine system theory can simply be taught in a lecture course without an accompanying laboratory,[2] which deprives students of hands-on experience. Second, the "virtual laboratory" approach allows students to run simulated experiments on computers programmed with gas turbine system models.[3] At its best, this approach can provide audio-visually rich reproductions of actual laboratory environments intended to mimic the physical reality of live laboratory testing. Nonetheless, the models and virtual experiments are prescribed and students still miss the pragmatic experience of applied, hands-on experimentation. Third, an experimental gas turbine laboratory apparatus, either expressly built using an available turbine or purchased through an educational manufacturer,[4] can showcase actual experimental operation of these systems. However, this approach is prohibitively expensive to most STEM programs that lack dedicated gas turbine research divisions.

To integrate hands-on energy topics, particularly gas turbines, into STEM curricula, we propose an alternative to creating virtual laboratories with no real hardware or investing in capitally-intensive lab equipment. An archive of "Energy Engineering Laboratory Modules" (EELMs) is being developed by collaborating faculty and students at MSOE, accumulated, and disseminated to facilitate spiral insertion of energy engineering concepts into college and high school courses across STEM curricula. EELMs are economical, hands-on, "turn-key" activities that can be incorporated into any STEM curricula to introduce energy studies. For example, a series of building energy audit exercises was recently created and described that harvests existing buildings as living laboratories suitable for quantitative evaluation using an inexpensive audit tool kit.[5] Additionally, a small, inexpensive inverted downdraft wood gasifier for processing pine chips into syngas was designed from a metal vacuum-flask-style thermos bottle. It was constructed for less than $50 to teach students about biomass-to-energy processes.[6]

To create EELM hardware for gas turbine experimentation, we propose constructing the disk turbine shown in Figure 1 using freely available instructions obtained on-line from the Instructables Web site.[7] This design uses platters harvested from obsolete computer hard drives,

which are often freely available at K-12 schools and colleges that periodically retire old computers. Hard drive platters can also be cheaply obtained from computer hardware reuse sites such as Craig's List.

Disk turbines (also called boundary layer turbines or Tesla turbines) differ from conventional aero-derived turbines. Instead of gas impinging on aerodynamic blade surfaces to produce lift and spin the shaft, disk turbines rely on viscous shear between the working fluid and flat disks to provide motive torque. As a result, disk turbines typically operate at much higher rotational rates with lower torque than their aero-derived counterparts, and they typically operate at a lower energy conversion efficiency.[8] Nonetheless, since complex aerodynamic blades need not be fabricated, disk turbines are extremely easy and inexpensive to create, making them ideal as centerpieces for a gas turbine EELM.

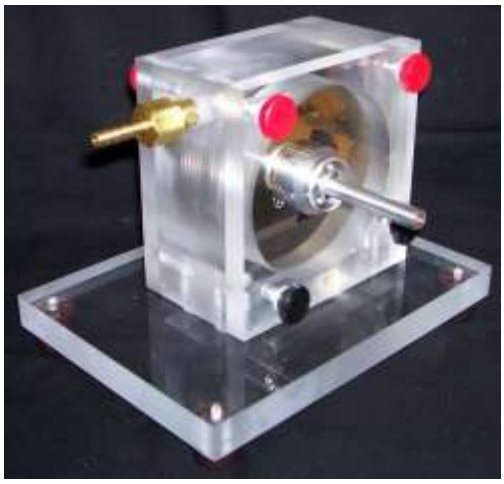

Figure 1: Students will build and test small disk turbines fabricated using discarded computer hard drive platters following Instructables guidelines. *This image was used under a Creative Commons convention; original at: http://www.instructables.com/file/FV0S7YD5AQEP27YAST*

Experimental evaluation of engines and turbo-machinery typically requires a dynamometer to measure power curves – power output as a function of rotational rate for a series of loads. Due to the high-rotation-rate and low torque output by disk turbines, no commercially-available dynamometers are suitable. Moreover, significant characterization is required to correctly design appropriate custom dynamometers, which are also expensive to build.[9] To avoid these costs and complications, we use a technique called dynamic dynamometry, which uses the rotational inertia of the turbine spindle and the friction in the bearings as the load. No separate dynamometer is needed to extract power curves. This technique has already been used successfully by researchers to characterize tiny disk turbines[10] and disk turbines for space applications.[11] We adapt it here for educational purposes.

Critical to our technique is determination of turbine rotational inertia. While rotational inertia can be measured or estimated through multiple different techniques already reported in the literature, we feel the dynamic dynamometer approach is superior in the context of educational labs. By contrast, in the Energy Method,[12] a light string attached to a weight of known mass is wound around the turbine shaft. The mas is released, and it falls until it hits the ground. The spindle is then allowed to spin down to rest. The turbine's rotational inertia is determined from an energy balance on the attached falling mass assuming friction in the bearings is constant with respect to rotational velocity. We showed through experimental measurement that this constant-bearing-friction assumption is invalid, suggesting that dynamic dynamometry can provide more accurate rotational inertia measurements than the Energy Method. In the Geometry Method, a theoretical formula is used to determine rotational inertia of a single rigid component of regular geometry.[13], [14] The drawbacks of this technique include need to break apart the turbine to measure its internal geometry and inability to correctly evaluate turbines with irregular or complex geometry. By

comparison, the advantage of dynamic dynamometry is accurate assessment of turbine rotational inertia with no knowledge of the turbine's internal structure.

We explain in this paper how dynamic dynamometry techniques can be taught in the context of four unique mechanical engineering classes: Dynamics, Numerical Methods, Thermodynamics, and Experimental Methods. Along the way, we weave together all the steps of the technique including measuring the turbine's rotational inertia, extracting power curves, and eliminating outliers from the data set. We suggest that these different experimental project components be conducted in several unique courses across a STEM program's curriculum. The benefits of showing different aspects of the same experimental project across multiple courses have already been illuminated in the literature.[15]

Experimental Demonstrations, Results, and Analysis

All experiments we describe use an inexpensive optical tachometer to enable continuous measurement of the turbine shaft rotation rate, and a video recording device (we used the free video capture feature on an iPhone). The video-recorded tachometer readout provides time histories of the turbine shaft angular velocity during experimental events, which is the fundamental data stream analyzed to extract turbine performance metrics.

To reduce data to useful form, free frame-by-frame video viewing software was utilized (we chose VLC Media Player[16]). The approximate data sampling rate was determined by placing a stopwatch in the video recorder's field of view and counting the number of frames shot over some characteristic duration. Each frame therefore shows the tachometer reading at a sampling interval equal to the frame rate of the video capture device used. An example of the entire set-up is shown in Figure 2.

Figure 2: Optical tachometer and stopwatch positioned in the same video shot to enable video capture of turbine spindle experimental rotational velocity time histories for data analysis.

Note that for future classroom deployment of the dynamic dynamometer EELMs, we plan to build and use the Instructable turbine shown in Figure 1. However, to develop and evaluate the underlying techniques described here, we saved time and resources by using a small pre-built disk turbine made available by an industry partner. While this hardware switch will affect numerical quantities measured and calculated (i.e., the pre-built turbine from industry has higher rotational inertia than the Instructable turbine), the underlying techniques can be universally applied to any disk turbine.

Dynamics Course: Turbine Rotational Inertia Determination by Dirac Force Input

One technique for disk turbine spindle moment of inertia determination can be demonstrated in a sophomore-level Dynamics course by applying particle kinematics and kinetics concepts universally taught in this course. For the demonstration, the turbine is anchored just above head

height. One end of a long, light string (we used sewing thread) is secured to the turbine spindle, and the other end is attached to a free weight of known mass resting at the elevation of the turbine. The shaft is then rotated by hand, allowing the string to wrap around the shaft without doubling up on itself. With video capture of tachometer data enabled, the weight is knocked to the floor, spinning the turbine shaft with an instantaneous input of force provided by gravity acting on the weight's mass.

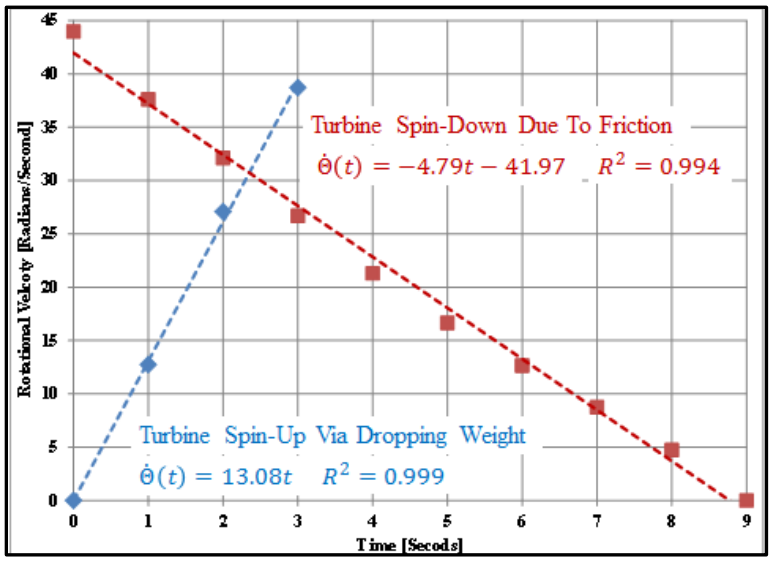

Figure 3: Experimental data for turbine spin-up under constant force imposed by a falling mass (blue data) and for spin down under bearing friction (red data). Fits to both experimental data sets show the underlying functions are highly linear; while not shown here due to figure scale, the spin-down trend was shown to be linear for starting rotational velocities as high as 404 radians/second.

An example of the resulting data is shown in Figure 3. Analyzing these data in conjunction with a free body diagram, shown in Figure 4, for the weight-string-turbine dynamic system results in an experimental measurement for turbine spindle rotational inertia.

In general, turbine spindle angular acceleration under inlet gas pressure, $\ddot{\Theta}_a(t)$, under a falling mass, $\ddot{\phi}_a(t)$, or deceleration due to bearing friction, $\ddot{\Theta}_d(t)$, are approximated via the time derivative of collected experimental angular turbine data,

$$\ddot{\Theta}(t) = \frac{\Delta\dot{\Theta}(t)}{\Delta t} \qquad \text{(Eq. 1)}$$

where $\dot{\Theta}(t)$ is the spindle angular velocity, and Δt is a time interval of measurement. Applying Newton's Second Law through a torque balance on the free body diagram in Figure 4, the difference between the torque imposed on the turbine shaft by the string, $F_s(D/2)$, and the frictional torque from the bearings, T_f, upon which the turbine spindle is mounted is given by

$$F_s\left(\frac{D}{2}\right) - T_f(t) = I \cdot \ddot{\phi}_a(t) \qquad \text{(Eq. 2)}$$

where I is the rotational inertia of the turbine spindle, F_s is the force of the string arising from the weight of the fixed mass, m, and D is the diameter of the spindle around which the thread is wound. Finally, by applying a dynamic force balance to the falling mass alone (see Figure 4), the following expression results,

$$m \cdot \ddot{\phi}_a(t) \cdot \left(\frac{D}{2}\right) = m \cdot g - F_s \qquad \text{(Eq. 3a)}$$

where g is the local gravitational acceleration. This expression can be solved for F_s:

$$F_s = m \cdot g - m \cdot \ddot{\phi}_a(t) \cdot \left(\frac{D}{2}\right) \quad \text{(Eq. 3b)}$$

To obtain an experimental function for T_f, the friction torque from the bearings, the unloaded turbine was spun up to its maximum operational rotational velocity using compressed air. When the turbine reached a steady state rate of rotation, the input gas was instantaneously shut off, and the rotational velocity of the turbine with respect to time was logged while the turbine spun down under friction primarily imposed by the bearings. A torque balance on the decelerating turbine spindle alone yields

$$-T_f(t) = I \cdot \ddot{\Theta}_d(t) \quad \text{(Eq. 4)}$$

where $\ddot{\Theta}_d(t)$ is determined from Equation 1. Substituting Eq. 4 into Eq. 2 and rearranging gives

$$I = \frac{F_s\left(\frac{D}{2}\right)}{\ddot{\phi}_a(t) - \ddot{\Theta}_d(t)} \quad \text{(Eq. 5)}$$

and plugging the F_s expression of Equation 3b into Equation 5 results in an expression to determine I values exclusively from experimentally-measured inputs,

$$I = \frac{\left[mg - m\ddot{\phi}_a(t)\frac{D}{2}\right]\left(\frac{D}{2}\right)}{\ddot{\phi}_a(t) - \ddot{\Theta}_d(t)} \quad \text{(Eq. 6)}$$

Now, to determine the value for I, the numerical values of the functions $\ddot{\phi}_a(t)$ and $\ddot{\Theta}_d(t)$ were found at each time step: t_1, t_2, … t_n. These values were plugged into Equation 6, which produced N-1 values for I where N is the total number of data points. The reported value for I is the average of all the discrete I values for each time step while the uncertainty in I is approximated as twice the standard deviation of all the data.

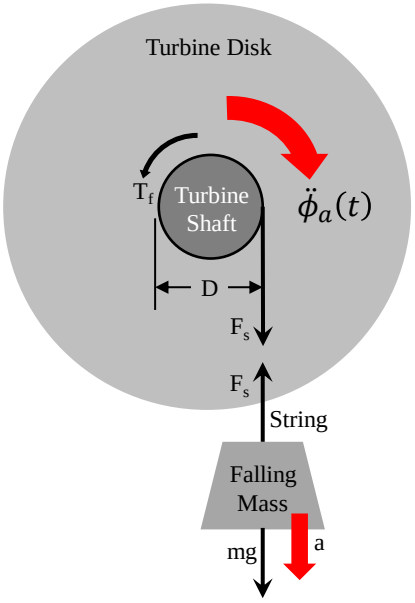

Figure 4: Free body diagram for weight-string-turbine system showing acceleration directions, forces, and torques acting on components.

<u>Numerical Methods Course: Turbine Rotational Inertia Determination by Torsion Spring</u>

The turbine spindle moment of inertia, I, can also be determined through an alternative experiment that uses an oscillating torsional spring instead of a falling mass. This technique, which uses numerical integration of rotational velocity data to obtain rotational position, can be taught in a junior-level Numerical Methods course to showcase a practical application of numerical integration.

A torsional spring is connected to the disk turbine apparatus

allowing for oscillatory dynamic analysis of this system. With the data-logging system running, the torsional spring is twisted to give an initial displacement to the system. Using Newton's Second Law, the governing differential equation is

$$I\ddot{\Theta} + \beta\dot{\Theta} + \kappa\Theta = 0 \qquad \text{(Eq. 9)}$$

where β is the coefficient of viscous friction; κ is the known torsional spring constant; and $\ddot{\Theta}$, $\dot{\Theta}$, and Θ are turbine angular acceleration, velocity, and displacement respectively. The major assumption for this experimental setup is that the frictional torque is viscous, $T_f = -\beta\dot{\Theta}$. The rotational velocity, $\dot{\Theta}$ in radians/second, measured using the tachometer, is numerically integrated to obtain the angular position, Θ in radians. Another option for the experimental setup would be to use an absolute encoder, if available, to measure the angular position of the shaft directly.

Using the angular position of the turbine shaft determined via either method described, students can determine the un-damped natural frequency, ω_n, and damping ratio, ζ, using the logarithmic decrement method. The natural frequency and damping ratio are related to the moment of inertia, I, the coefficient of viscous friction, β, and the torsional spring constant, κ, by

$$\omega_n = \sqrt{\kappa/I} \qquad \text{(Eq. 10)}$$

and

$$\zeta = \frac{\beta}{2\sqrt{\kappa I}} \qquad \text{(Eq. 11)}$$

The moment of inertia can then be found from the two equations with two unknowns (I,β).

If both methods for determining turbine spindle rotational inertia are presented to a single class, the students can then compare the results from each method while discussing the merits and drawbacks of each. Furthermore, since the Instructable disk turbine can be disassembled, each spindle part can be weighed, and their dimensions measured. The resulting rotational inertia can then be built up analytically by superposition as an additional point of comparison and discussion. Students typically learn this technique in Dynamics but are rarely able to practically test it in that course.

Thermodynamics Course: Turbine Power Curve

Turbine power output as a function of rotational velocity, the so-called turbine power curve, can be extracted experimentally by dynamic dynamometry. If the pressure at which compressed air is input to the turbine is modulated by a regulator, a family of power curves can be produced, showing the turbine's power output for a range of input pressures. Finally, if a volume flow rate meter is integrated into the gas line, the ratio of turbine power output to the total energy input gives turbine energy conversion efficiency. All of these aspects of turbine performance can be taught in a junior- or senior-level Thermodynamics course.

To illustrate turbine power curve measurement, we ran the turbine shown in Figure 2 using a range of input pressures: 90 psi, 80 psi, 70 psi, 60 psi, 50 psi, and 40 psi. Pressure upstream of the turbine was held constant using a regulator. While higher and lower pressures were available, we deemed 100 psi too high for safe disk turbine operation. We also found that the turbine would not spin up on its own for input pressures less than 30 psi. Increments of 10 psi were used for convenience because the resulting power curves are easily distinguished from one another and the regulator pressure gauge used read out in 10 psi increments.

To perform necessary data acquisition in a lecture or lab course, the pressure regulator is set to a desired preset value. Video capture of tachometer data is initiated with the turbine at rest. The turbine gas inlet is instantaneously opened, and the turbine is allowed to spin up until its rotational velocity reaches steady state (we describe later how 'steady state' is formally defined). To get a 'feel' for steady-state operation, during the turbine spin-up process, the bearings will audibly whir. The pitch will continue to grow higher as the turbine accelerates. When the pitch of the turbine's audible whir stops increasing, this is a qualitative indication that steady state rotational velocity has been reached. To ensure steady state was, in fact, achieved in all our data sets, each experiment was allowed to proceed for 60 seconds beyond the time indicated by a steady pitch in the turbine's audible whir. The resulting experimental data is shown in Figure 5 for 90 psi input pressure.

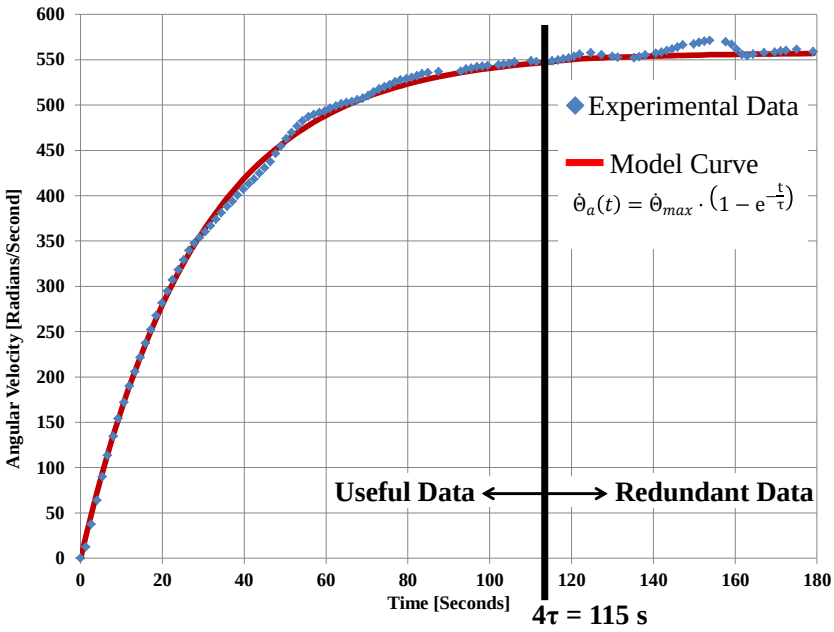

Figure 5: Rotational velocity versus time for a disk turbine spun up from rest at constant input pressure. The experimental data (blue diamonds) follow an asymptotic exponential, Equation 11, (red curve) where the system time constant, τ, must be selected to provide the best data/model fit. Data collected after time = 4τ are redundant and can be eliminated from the analysis.

The following derivation leads to a turbine power curve expression. The turbine's moment of inertia, *I*, is already known from the above-described analysis in the Dynamics and Numerical Methods courses. The turbine's power output, P_{out}, is

$$P_{out} = T_{out} \cdot \dot{\Theta}_a(t) = I \cdot \frac{d\dot{\Theta}_a(t)}{dt} \cdot \dot{\Theta}_a(t) \qquad \text{(Eq. 9)}$$

since the output shaft torque, T_{out}, is

$$T_{out} = I \cdot \frac{\mathrm{d}\dot{\Theta}_a(t)}{\mathrm{d}t} \qquad \text{(Eq. 10)}$$

To find an equation for P_{out}, a functional form is needed for $\dot{\Theta}_a(t)$. This function can be determined by inspection. An example raw $\dot{\Theta}_a(t)$ data set is given in Figure 5, and it is apparent from the non-zero initial slope that the functional for $\dot{\Theta}_a(t)$ is a first order response (an asymptotic exponential) of the form

$$\dot{\Theta}_a(t) = \dot{\Theta}_{max} \cdot \left(1 - \mathrm{e}^{-\frac{\mathrm{t}}{\tau}}\right) \qquad \text{(Eq. 11)}$$

where $\dot{\Theta}_{max}$ is the maximum turbine rotational velocity achieved at steady-state, and τ is a time constant characteristic of the system.

To fit Equation 11 to the experimental data and obtain a useful functional for $\dot{\Theta}_a(t)$, the time constant, τ, is treated as a variable parameter that is adjusted to achieve the best equation/experiment match. The fitting technique we used was minimization of the Standard Error of the Estimate (SEE). SEE is the sum of all the absolute differences between model and experiment at each discrete time step. Figure 5 shows the exceptional experiment/model fit between real data and Equation 11 when τ is selected to minimize SEE.

Identifying the correct value for τ enables further useful data reduction by approximating the time at which turbine steady state rotation rate was achieved. All data collected after this time can be discarded as redundant. We used 4τ as the number of time constants required for the system to reach steady state. This decision is justified via the following analysis. At time = 0, $\dot{\Theta}_a(0) = 0$. For a functional form of $\dot{\Theta}_a(t) = \dot{\Theta}_{max}\left(1 - \mathrm{e}^{-\frac{\mathrm{t}}{\tau}}\right)$, at time = 4τ, $\dot{\Theta}_a(4\tau) = \dot{\Theta}_{max}\left(1 - \mathrm{e}^{-\frac{4\tau}{\tau}}\right) \approx 0.982 \cdot \dot{\Theta}_{max}$. At time $\rightarrow \infty$, $\dot{\Theta}_a(\infty) \rightarrow \dot{\Theta}_{max}$. Therefore, the percent error of $\dot{\Theta}_a(4\tau)$ at time = 4τ relative to $\dot{\Theta}_{max}$ at time $\rightarrow \infty$ is given by the following calculation:

$$\% = \frac{\dot{\Theta}_{max} - \dot{\Theta}_a(4\tau)}{\dot{\Theta}_{max}} = \frac{\dot{\Theta}_{max} - (98.2\%)\dot{\Theta}_{max}}{\dot{\Theta}_{max}} \approx 1.8\% \qquad \text{(Eq. 12)}$$

In other words, the percent error of $\dot{\Theta}_a(4\tau)$ relative to $\dot{\Theta}_{max}$ is less than 2%, which we deem to be an acceptable engineering approximation in characterizing this system. If additional error reduction is desired, data can be retained for a duration of $n\tau$ where n is an arbitrary number selected based on the level of precision needed for calculations.

Given the experimentally determined functional form of $\dot{\Theta}_a(t)$ in Equation 11, the turbine output power, P_{out}, can be expressed by carrying out the derivative implied in Equation 9

$$P_{out} = I \cdot \frac{d\dot{\Theta}_a(t)}{\mathrm{d}t} \cdot \dot{\Theta}_a(t) = I \frac{d\left[\dot{\Theta}_{max}\left(1 - \mathrm{e}^{-\frac{\mathrm{t}}{\tau}}\right)\right]}{dt} \dot{\Theta}_a(t) = \frac{I}{\tau} \cdot \dot{\Theta}_a(t) \cdot \dot{\Theta}_{max} \cdot \mathrm{e}^{-\frac{\mathrm{t}}{\tau}} \qquad \text{(Eq. 13)}$$

which reduces through the following algebraic manipulations to a second-order polynomial equation:

$$P_{out} = \frac{I}{\tau} \cdot \dot{\Theta}_a(t) \cdot \left[\dot{\Theta}_{max} - \dot{\Theta}_{max} + \dot{\Theta}_{max} \cdot e^{-\frac{t}{\tau}}\right] \quad \text{(Eq. 14a)}$$

$$P_{out} = \frac{I}{\tau} \cdot \dot{\Theta}_a(t) \cdot \left[\dot{\Theta}_{max} - \dot{\Theta}_{max} \cdot \left(1 - e^{-\frac{t}{\tau}}\right)\right] \quad \text{(Eq. 14b)}$$

$$P_{out} = \frac{I}{\tau} \cdot \dot{\Theta}_a(t) \cdot \left[\dot{\Theta}_{max} - \dot{\Theta}_a(t)\right] \quad \text{(Eq. 14c)}$$

Therefore, the power output final formula is obtained,

$$P_{out} = \frac{I}{\tau} \cdot \left[\dot{\Theta}_{max} \cdot \dot{\Theta}_a(t) - \dot{\Theta}_a(t)^2\right] \quad \text{(Eq. 14d)}$$

For a particular compressed air input pressure, experimental values for τ and $\dot{\Theta}_{max}$ are determined using techniques described above. The representaive emperical turbine power curve of Equation 14d can be plotted for the series of rotataional velocities measured at each discrete time step during turbine spin-up. Figure 6 shows a family of example power curves for the disk turbine of Figure 2 over the following range of input pressures: 90 psi, 80 psi, 70 psi, 60 psi, 50 psi, and 40 psi.

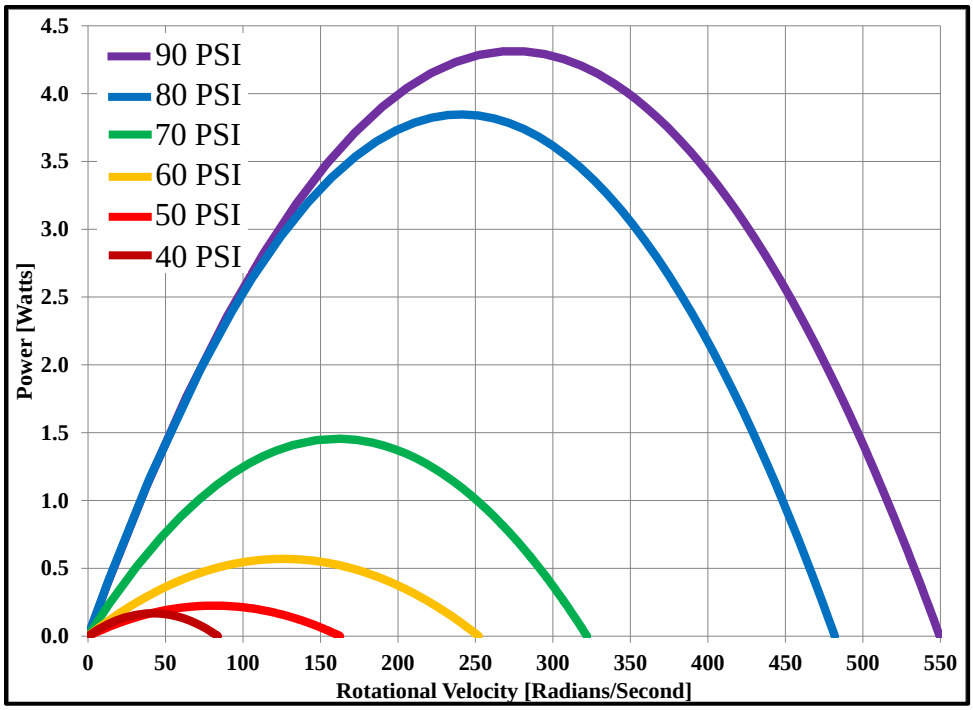

Figure 6: A family of power curves representing Equation 14d extracted through empirical dynamic dynamometry measurements using an unloaded disk turbine operating over a range of input pressures.

Another imporant question relevant to Thermodynamics is how well the emperical power curve model of Equation 14d matches the turbine's actual performance. The most direct approach would be to attatch a dynamometer to the turbine to experimentally extract a measured power curve. However, as stated above, disk turbines require expensive customized dynamometers whose creation is beyond the scope of a STEM program without a specilized turbine research division. As an alternative, therefore, it is reasonable to extract power data directly from dynamic dynamomtry by using an approximate differential form of Equation 9.

$$P_{out} \approx I \cdot \frac{\Delta \dot{\Theta}_a(t)}{\Delta t} \cdot \dot{\Theta}_a(t) \qquad \text{(Eq. 15)}$$

Here, the differential rotational velocity measured during turbine spin-up at each time step substitues for the pure derivative allowing the turbine power output at each rotational velocity to be quantified. An example of the resulting comparision between the emperical power curve model of Equation 11 and the discrete turbine power versus rotational velocity represented by Eqauation 15 is shown in Figure 7 for the representative case of 90 psi compressed gas inlet pressure.

Experimental Methods Course: Data Outlier Elimination

Once the empirical power curve model and discrete turbine power versus rotational velocity are available, the match between model and experimental data and the data's quality can be evaluated. In engineering curricula, the analytical tools to make this type of assessment are typcially taught in Experimental Methods courses, but the analysis could also be framed in the context of a mathematics course in Statisitics.

Model/Experiment agreement can be visually qualitatively evalauted by plotting both sets together, as is shown in Figure 7 for the representative case of 90 psi turbine inlet pressure. The experimetnal data follow the same second order polynomial curve as the model with the $\dot{\Theta}_a(t)$ for both maximum power and for when output power is extinguished, which occur respectively at rotational velocities similar to those predicted by the model. To gain further insight, the data can be fitted with a quadratic regression (we added this trend using embedded tools in Microsoft Excel – see Figure 7), which illustrates the second-order curve best fitting the data. Owing to the coarse data acquisition frequency and the need for manual data input, the experiment is prone to instances of random error. This susceptibility provides an educational opportunity to demonstrate how to identify possible outliers and apply statistical techniques to decide whether they can be legitimately eliminated from the data set.

For each data point, we calculated the absolute difference between output power determined experimetnally and output power suggested by the best-fit polynomial for the data. These differences were then averaged to obtain $\overline{\dot{\Theta}_a}$, and their standard deviation, $\sigma_{\dot{\Theta}_a}$, was calculated. The farthest outlying point was then interrogated using Chauvenet's Criterion,[17]

$$Z = \frac{\left|\overline{\dot{\Theta}_a} - \dot{\Theta}_a(t)\right|}{\sigma_{\dot{\Theta}_a}} \qquad \text{(Eq. 16)}$$

where Z is the number of standard deviations by which the suspect outlier differs from the average. Then $\mathcal{P}(Z)_{out}$ is evaluated using a normal error integral of a Gaussian distribution; $\mathcal{P}(Z)_{out}$ is the probability that a legitimate measurement will differ from $\overline{\dot{\Theta}_a}$ by a magnitude of Z or more standard deviations. If it is found that

$$N \cdot \mathcal{P}(Z)_{out} < 0.5 \qquad \text{(Eq. 17)}$$

where N is the total number of measurements taken before an elapsed time of 4τ, then the suspect outlying data point is thrown out.

The quadratic regression is then re-fitted to the remaining data, a new average and standard deviation are calculated, and the the next farthest outlying point is evaluated via the process above. Outlier elimination continues until all remaining data points satisfy Chauvenet's Criterion. Figure 7 shows the progression of quadratic regression curve fits to the experimental data as outliers failing Chauvenet's Criterion are eliminated. As outliers are eliminated, agreement between the experimental curve fit and turbine output power predicted by Equation 14d continues to improve, further justifying this elimination process.

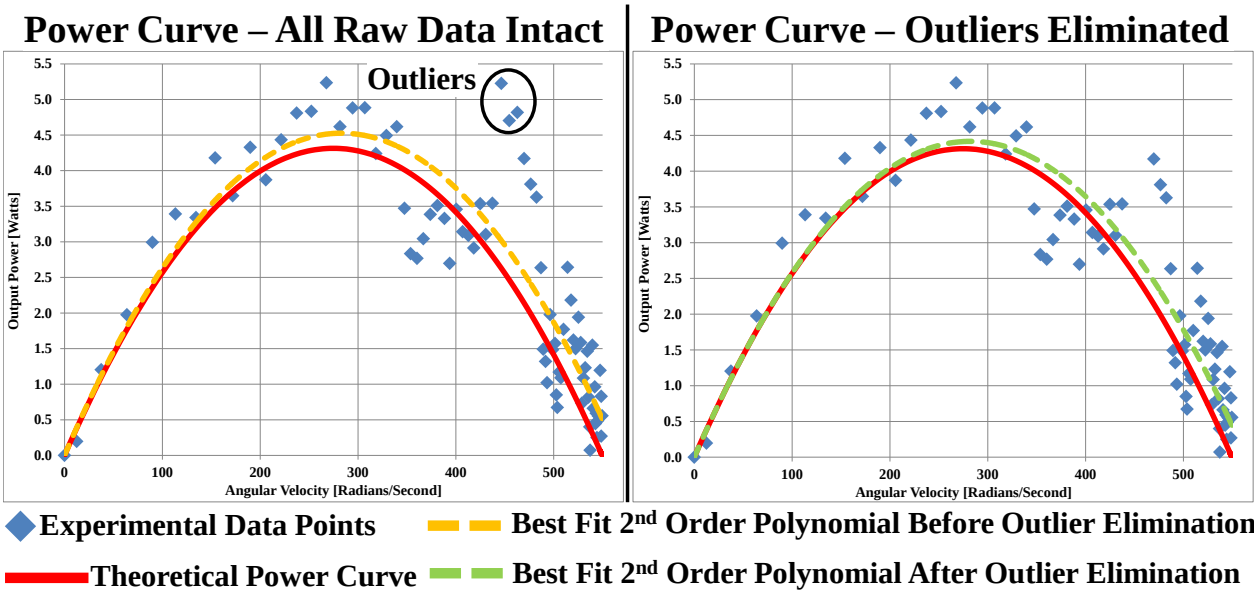

Figure 7: Example theoretical versus experimental turbine power curves obtained from dynamic dynamometry. (Left) With all raw data intact, the fitted polynomial over-predicts performance; outlying data failing Chauvenet's criterion are encircled in black. (Right) By removing outlying data points, the resulting theoretical/experimental agreement is further improved.

An important interpretive and educational question to ask is: how much does the outlier elimination process actually move the fitted curve? In other words: how much do the outliers impact the turbine's predicted performance? Of paramount importance to turbine evaluation is predicting and operating at peak power and identifying the rotational velocity that maximizes this output power. For the disk turbine we characterized operating at 90 psi inlet pressure, the predicted peak power output was about 4.53 Watts before removing outliers. After outlier elimination, the predicted peak power fell to about 4.42 Watts, a 2.49% difference in power output. This difference is probably not large enough to be concerning from a practical engineer's perspective, but it is large enough to show difference in magnitude and position of the fitted curve before and after outlier elimination. Perhaps of greatest value in an Experimental Methods course is that this random-error-prone experiment allows students to actually use Chauvenet's Criterion in a real application to eliminate outliers. Most of the time (at least in our anecdotal laboratory teaching experience), students do not get to practice a formal technique to eliminate outliers because lab experiments are usually well-tuned so as not to produce anomalies. Often,

students want to throw out data points because they do not "look right" or they do not match the theory. Applying Chauvenet's Criterion to real data gives students a formal toolset to quantitatively evaluate the validity of data points that look suspicious.

Conclusion

Within STEM curricula, a need exists to provide practical, hands-on training in gas turbine systems while keeping institutional costs and additional program credit hours manageable. Presented here is a method to accurately measure and predict the mechanical power output of a small disk turbine running on compressed air that requires minimal, inexpensive, and easily accessible equipment. The disk turbine itself is extremely easy and inexpensive to create making it an ideal centerpiece for a gas turbine EELM. To avoid need to purchase or build a custom dynamometer, we showcase a technique called dynamic dynamometry, which requires only an inexpensive optical tachometer, a digital video recorder, and free image capture software for data acquisition.

The dynamic dynamometry techniques can be taught through four unique mechanical engineering classes: Dynamics, Numerical Methods, Thermodynamics, and Experimental Methods. The disk turbine's rotational inertia can be measured experimentally using knowledge and skills typically taught in undergraduate courses in Dynamics and Numerical Methods. In the context of a junior- or senior-level Thermodynamics course, we show how to derive the power curve equation for a turbine, eliminate redundant data, and use the remaining data to correctly fit a single empirical parameter to define power curves. Finally, we show how outliers among the data can be identified and eliminated via statistical techniques that would be taught in a junior- or senior-level Experimental Methods course.

Acknowledgements

We gratefully acknowledge EASENET, Inc. for project financial and material support as well as the Wisconsin Space Grant Consortium 2012-2013 Higher Education Incentives Award Program for financial support. This paper's undergraduate lead author is a member of the Milwaukee Undergraduate Researcher Incubator (MURI) at MSOE, an organization which fast-tracks undergraduates into meaningful early research experiences.

Bibliography

[1] L. S. Langston, "The Adaptable Gas Turbine," *American Scientist*, Vol. 101, July-August 2013, pp. 264-267.
[2] W. A. Woods, P. J. Bevan, D. I. Bevan, "Output and Efficiency of the Closed-Cycle Gas Turbine," *Proceedings of the Institution of Mechanical Engineers, Part A: Journal of Power and Energy*, Vol. 205, No. 1, February 1991, pp. 59-66.
[3] K. Mathioudakis, N. Aretakis, P. Kotsiopoulos, E. A. Yfantis, "A virtual laboratory for education on gas turbine principles and operation," ASME paper GT2006-90357, *Proceedings of the 2006 ASME Turbo Expo: Power for Land, Sea, and Air*, Barcelona, Spain, May 8-11, 2006.
[4] Turbine Technologies, LTD., "MiniLab™ Gas Turbine Lab," URL: http://www.turbinetechnologies.com/EducationalLabProducts/TurbojetEngineLab.aspx, accessed 7/27/2013.

[5] M. J. Traum, "Harvesting Built Environments for Accessible Energy Audit Training," *Proceedings of the 2nd International Conference on the Constructed Environment*, Chicago, IL, October 29-30, 2011.
[6] M. J. Traum, J. A. Anderson, K. Pace, "An Inexpensive Inverted Downdraft Biomass Gasifier for Experimental Energy-Thermal-Fluids Demonstrations," *Proceedings of the 120th American Society for Engineering Education (ASEE) Conference and Exposition*, Atlanta, GA, June 23-26, 2013.
[7] Instructables Web Site, "Build a 15,000 rpm Tesla Turbine using hard drive platters," URL: http://www.instructables.com/id/Build-a-15,000-rpm-Tesla-Turbine-using-hard-drive-/, accessed 7/23/2013.
[8] T. A. Emran, "Tesla Turbine Torque Modeling for Construction of a Dynamometer and Turbine," M.S. Thesis, University of North Texas, May 2011.
[9] T. A. Emran, R. C. Alexander, C. T. Stallings, M. A. DeMay, M. J. Traum, "Method to Accurately Estimate Tesla Turbine Stall Torque for Dynamometer or Generator Load Selection," *ASME Early Career Technical Journal*, Vol. 10, pp. 158-164, 2010 [URL: http://districts.asme.org/DistrictF/ECTC/2010ECTC.htm].
[10] V. G. Krishnan, Z. Iqbal, M. M. Maharbiz, "A micro Tesla turbine for power generation from low pressure heads and evaporation driven flows," *Proceedings of the 16th International Solid-State Sensors, Actuators and Microsystems Conference*, June 5-9, 2011, Beijing, China, pp. 1851-1854.
[11] Z. Yang, H. L. Weiss, M. J. Traum, "Dynamic Dynamometry to Characterize Disk Turbines for Space-Based Power," *Proceedings of the 23rd Annual Wisconsin Space Conference*, Milwaukee Wisconsin, August 15-16, 2013.
[12] A. Mishra, Practical Physics for Engineers, Firewall Media, 2006.
[13] Kruger Ventilation, "Starting Torque of Fan," TBN019.1/2001, URL: http://www.krugerfan.com/brochure/publications/Tbn019.pdf, accessed 9/8/2013.
[14] B. Bolund, H. Bernhoff, M. Leijon. "Flywheel energy and power storage systems," *Renewable and Sustainable Energy Reviews*, Volume 11, Number 2, 2007, pp. 235-258.
[15] M. J. Traum, V. Prantil, W. Farrow, H. Weis, "Enabling Mechanical Engineering Curriculum Interconnectivity Through An Integrated Multicourse Model Rocketry Project," *Proceedings of the 120th American Society for Engineering Education (ASEE) Conference and Exposition*, Atlanta, GA, June 23-26, 2013.
[16] VCL Media Player, URL: http://www.vlcapp.com/vlc-features/frame-by-frame-video-player/ , accessed 7/30/2013.
[17] J. R. Taylor, An Introduction to Error Analysis The Study of Uncertainties in Physical Measurements, 2nd Ed., University Science Books, Sausalito, CA, 1997.